Diiron and Dicobalt Complexes of a Phenolate-Bridged Binucleating Ligand with Mixed Phenolate and Pyridine Podands

V. D. Campbell, E. J. Parsons,* and W. T. Pennington

Department of Chemistry, Clemson University, Clemson, South Carolina 29634-1905

The ligand 2,6-bis{[(2-hydroxyphenyl)(2-pyridylmethyl)amino]methyl}-4-methylphenol (H_3L) was synthesized, and its crystal structure was determined. Crystal data for H_3L: triclinic space group $P\bar{1}$ (No. 2), $a = 8.935(3)$ Å, $b = 12.376(4)$ Å, $c = 13.843(4)$ Å, $\alpha = 73.21(2)°$, $\beta = 88.05(2)°$, $\gamma = 81.91(3)$, $V = 1450.7(8)$ Å^3, and $Z = 2$. The structure was refined to $R = 0.064$ ($R_w = 0.078$) for 2117 data with $I > 3\sigma(I)$. Reaction of this ligand with $CoCl_2$ and $NaO_2CCH_2CH_3$ yielded the dicobaltic complex $[Co_2L(O_2CCH_2CH_3)_2]^+$. A crystal structure determination of the tetraphenylborate salt of this complex reveals that the two cobalt atoms are bridged by the central phenolate group of the ligand and that each cobalt atom is further chelated by three remaining donor sites of the septadentate ligand. The octahedral coordination sphere of each of the cobalt atoms is completed by two bridging propionate ligands. Crystal structure data for $[LCo_2(OPr)_2]BPh_4$: monoclinic space group $C2/c$ (No. 15), $a = 41.123(18)$ Å, $b = 11.469(5)$ Å, $c = 30.576(14)$ Å, $\beta = 120.95(3)°$, $V = 12368(8)$ Å^3, and $Z = 8$. The structure was refined to $R = 0.058$ ($R_w = 0.069$) for 4067 data with $I > 3\sigma(I)$. Reaction of the same ligand with $FeCl_2$ or $FeCl_3$ yielded the analogous diferric complex, $[Fe_2L(O_2CCH_2CH_3)_2]^+$. Oxidation proceeded very rapidly in the case of the iron complex, while the cobalt oxidation occurred much more slowly. A comparison of the structures of the free and coordinated ligand indicates that complexation proceeded with inversion at one of the tertiary amine junctures.

Introduction

Dimetallic complexes of several polypodal, binucleating ligand systems have been synthesized as models for metalloproteins.[1-3] These septadentate ligands incorporate a phenoxide or an alkoxide bridge and also provide three additional donor sites to each metal ion. The bridge functions to maintain the two metal centers in close proximity under conditions where simple oxo-bridged complexes are known to dissociate.[2,4] Some examples of polypodal ligands include *N,N'*-(2-hydroxy-5-methyl-1,3-xylylene)bis[*N*-(carboxymethyl)glycine] (HXTA),[5] 2,6-bis[(bis(2-pyridylmethyl)amino)methyl]-4-methylphenol (HBPMP),[6] 2,6-bis{[[2-(1-pyrazolyl)ethyl][2-(2-pyridyl)ethyl]amino]methyl}-4-methylphenol,[7] 2,6-bis[(bis(1-methylimidazol-2-ylmethyl)amino)methyl]-4-methylphenol (Hbimp),[3] 2,6-bis[(bis(2-benzimida-zolylmethyl)amino)methyl]-4-methylphenol (HLBzim),[6] and *N,N,N',N'*-tetrakis(2-benzimidazolylmethyl)-2-hydroxy-1,3-di-aminopropane (TBPO).[1g]

Diiron complexes of these ligands have been examined as models for iron–oxo proteins such as hemerythrin (oxygen transport), methane monooxygenase (oxygen atom transfer), and purple acid phosphatases (phosphate level regulation).[1-3] Corresponding cobalt-containing enzymes, and therefore dicobalt complexes of the polypodal ligands, are less prevalent. However, cobalt complexes of ligands such as HBPMP have been reported as models for the copper-based, oxygen-transport enzyme hemocyanin.[1g,6]

Metalloprotein model complexes based on these multidentate ligands are chemically active, and have been shown in some instances to mimic the enzymes by reversibly binding oxygen[6] or by acting as oxygenation catalysts.[1b,h,8] We are attempting to extend this activity beyond the realm of enzymatic chemistry and into the binding and activation of small molecules in general. In doing so, we are not limited to polypodal ligands which mimic the coordination spheres of the various enzymes. Instead, we are interested in ligands having up to four different podands with which to manipulate and control the properties of the metal-binding sites.

Most current polypodal ligands contain only one type of podand. Two exceptions are 2,6-bis{[[2-(1-pyrazolyl)ethyl][2-(2-pyridyl)-ethyl]amino]methyl}-4-methylphenol,[7] which contains mixed pyridine and pyrazole donors, and 2-[(bis(2-pyridylmethyl)ami-no)-methyl]-6-[(benzyl)(2-pyridylmethyl)amino]methyl-4-methylphenol,[9] which contains three pyridine donors and one

(1) (a) Murch, B. P.; Boyle, P.; Que, L., Jr. *J. Am. Chem. Soc.* **1985**, *107*, 6728. (b) Murch, B. P.;; Bradley, F. C.; Que, L., Jr. *J. Am. Chem. Soc.* **1986**, *108*, 5027. (c) Suzuki, M.; Oshio, H.; Uehara, A.; Endo, K.; Yanaga, M.; Kida, S.; Saito, K. *Bull. Chem. Soc. Jpn.* **1988**, *61*, 3907. (d) Suzuki, M.; Uehara, A.; Oshio, H.; Endo, K.; Yanaga, M.; Kida, S.; Saito, K. *Bull. Chem. Soc. Jpn.* **1987**, *60*, 3547. (e) Borovik, A. S.; Murch, B. P.; Que, L., Jr. *J. Am. Chem. Soc.* **1987**, *109*, 7190. (f) Chen, Q.; Lynch, J. B.; Gomez-Romero, P.; Ben-Hussein, A.; Jameson, G.; O'Connor, C. J.; Que, L., Jr. *Inorg. Chem.* **1988**, *27*, 2673. (g) Sakurai, T.; Kaji, H.; Nakahara, A. *Inorg. Chim. Acta* **1982**, *67*, 1. (h) Nishida, Y.; Takeuchi, M.; Shimo, H.; Kida, S. *Inorg. Chim. Acta* **1984**, *96*, 115.

(2) (a) Borovik, A. S.; Hendrich, M. P.; Holman, T. R.; Münck, E.; Papaefthymiou, V.; Que, L., Jr. *J. Am. Chem. Soc.* **1990**, *112*, 6031. (b) Borovik, A. S.; Papaefthymiou, V.; Taylor, L. F.; Anderson, O. P.; Que, L., Jr. *J. Am. Chem. Soc.* **1989**, *111*, 6183. (c) Borovik, A. S.; Que, L., Jr. *J. Am. Chem. Soc.* **1988**, *110*, 2345.

(3) (a) Mashuta, M. S.; Webb, R. J.; McCusker, J. K.; Schmitt, E. A.; Oberhausen, K. J.; Richardson, J. F.; Buchanan, R. M.; Hendrickson, D. N. *J. Am. Chem. Soc.* **1992**, *114*, 3815. (b) Mashuta, M. S.; Webb, R. J.; Oberhausen, K. J.; Richardson, J. F.; Buchanan, R. M.; Hendrickson, D. N. *J. Am. Chem. Soc.* **1989**, *111*, 2745.

(4) (a) Hartman, J. R.; Rardin, R. L.; Chaudhuri, P.; Pohl, K.; Wieghardt, K.; Nuber, B.; Weiss, J.; Papaefthymiou, G. C.; Frankel, R. B.; Lippard, S. J. *J. Am. Chem. Soc.* **1987**, *109*, 7387. (b) Murray, K. S. *Coord. Chem. Rev.* **1974**, *12*, 1.

(5) Schwarzenbach, G.; Andregg, G.; Sallmann, R. *Helv. Chim. Acta* **1952**, *35*, 1785.

(6) (a) Suzuki, M.; Kanatomi, H.; Murase, I. *Bull. Chem. Soc. Jpn.* **1984**, *57*, 36. (b) Suzuki, M.; Ueda, I.; Kanatomi, H.; Murase, I. *Chem. Lett.* **1983**, 185. (c) Suzuki, M.; Kanatomi, H.; Murase, I. *Chem. Lett.* **1981**, 1745.

(7) Sorrell, T. N.; Vankai, V. A. *Inorg. Chem.* **1990**, *29*, 1687.

(8) For oxidations by some diiron complexes of nonpolypodal ligands, see: (a) Stassinopoulos, A.; Caradonna, J. P. *J. Am. Chem. Soc.* **1990**, *112*, 7071. (b) Jacob, M.; Bhattacharya, P. K.; Ganeshpure, P. A.; Satish, S.; Sivaram, S. *Bull. Chem. Soc. Jpn.* **1989**, *62*, 1325.

(9) Scheer, C.; Moneta, W.; Bardet, M.; Latour, J. M. *Abstracts of Papers*, 203rd National Meeting of the American Chemical Society, San Francisco, CA; American Chemical Society: Washington, DC, 1992; INOR 549. For a related ligand, see: Crane, J. D.; Fenton, D. E.; Latour, J. M; Smith, A. J. *J. Chem. Soc., Dalton Trans.* **1991**, 2979.

(10) Abbreviations: H_3L, 2,6-bis{[(2-hydroxyphenyl)(2-pyridylmethyl)ami-no]methyl}-4-methylphenol; OPr, propionate; BPMP, 2,6-bis[(bis(2-pyridylmethyl)amino)methyl]-4-methylphenolate; SCE, standard calomel electrode.

Table I. Crystallographic Data for H_3L and $[LCo_2(OPr)_2]BPh_4$

	H_3L	$[LCo_2(OPr)_2]BPh_4$
formula	$C_{33}H_{33}N_4O_{3.5}$	$C_{69}H_{64}BN_4O_7ClCo_2$
fw	541.65	1225.42
space group	$P\bar{1}$ (No. 2)	$C2/c$ (No. 15)
a, Å	8.935(3)	41.123(18)
b, Å	12.376(4)	11.469(5)
c, Å	13.843(4)	30.576(14)
α, deg	73.21(2)	
β, deg	88.05(2)	120.95(3)
γ, deg	81.91(3)	
V, Å^3	1450.7(8)	12368(8)
ρ_{calcd}, g cm^{-3}	1.24	1.32
μ(Mo Kα), mm^{-1}	0.08	0.63
transm coeff	0.92–1.00	0.88–1.00
R^a	0.064	0.058
$R_w{}^b$	0.078	0.069

$^a R = \sum \lVert F_o \rvert - \lvert F_c \rvert / \sum \lvert F_o \rvert.$ $^b R_w = [\sum w(\lvert F_o \rvert - \lvert F_c \rvert)^2 / \sum w \lvert F_o \rvert^2]^{1/2};$ $w = 1/[\sigma^2 F_o + g F_o{}^2].$

Table II. Atomic Coordinates ($\times 10^4$) and Equivalent Isotropic Thermal Parameters (Å$^2 \times 10^3$) for H_3L

	x	y	z	$U(eq)^a$
O(1)	2264(5)	10937(3)	2614(3)	72(2)
O(2)	4139(6)	13423(4)	1803(3)	97(2)
O(3)	3106(5)	10004(3)	1025(3)	87(2)
O(4)^b	−675(13)	4709(8)	4673(9)	128(6)
N(1)	1699(6)	13159(4)	3049(3)	63(2)
N(2)	952(8)	13021(5)	1220(4)	106(3)
N(3)	2805(5)	8445(3)	2849(3)	50(2)
N(4)	−381(7)	6859(5)	3330(4)	92(3)
C(1)	2407(6)	10578(5)	3645(4)	58(3)
C(2)	1747(6)	11248(5)	4247(5)	60(3)
C(3)	1938(7)	10808(5)	5284(5)	64(3)
C(4)	2761(7)	9747(5)	5726(5)	66(3)
C(5)	3401(7)	9128(5)	5087(5)	63(3)
C(6)	3244(6)	9514(5)	4051(4)	53(2)
C(7)	2923(9)	9282(6)	6856(5)	91(3)
C(8)	828(7)	12389(5)	3789(5)	68(3)
C(9)	3059(7)	13446(4)	3384(4)	60(3)
C(10)	4250(9)	13567(5)	2723(5)	74(3)
C(11)	5602(9)	13829(5)	3000(6)	87(3)
C(12)	5722(9)	13992(6)	3937(6)	95(4)
C(13)	4536(10)	13871(5)	4598(5)	85(3)
C(14)	3195(8)	13607(5)	4323(5)	72(3)
C(15)	721(7)	14135(5)	2400(5)	78(3)
C(16)	92(8)	13838(5)	1514(5)	70(3)
C(17)	−1227(8)	14377(6)	1051(5)	79(3)
C(18)	−1730(9)	14068(8)	250(6)	98(4)
C(19)	−865(11)	13201(8)	−42(6)	105(4)
C(20)	454(12)	12723(7)	438(6)	119(4)
C(21)	3953(6)	8805(5)	3397(4)	59(2)
C(22)	3456(6)	8052(5)	2017(4)	48(2)
C(23)	3595(6)	8869(5)	1131(4)	60(3)
C(24)	4157(7)	8586(6)	283(5)	77(3)
C(25)	4647(7)	7430(6)	357(5)	74(3)
C(26)	4506(7)	6607(6)	1232(5)	70(3)
C(27)	3893(6)	6910(5)	2075(4)	58(2)
C(28)	1795(6)	7743(5)	3486(4)	59(2)
C(29)	355(7)	7744(6)	2918(5)	64(3)
C(30)	−144(7)	8630(7)	2087(5)	80(3)
C(31)	−1496(9)	8621(9)	1621(6)	107(4)
C(32)	−2246(10)	7699(11)	2048(9)	120(6)
C(33)	−1736(10)	6857(9)	2869(8)	109(5)

^{a} Equivalent isotropic U defined as one-third of the trace of the orthogonalized U_{ij} tensor. ^{b} Half-occupancy atom.

noncoordinating benzene. We have now synthesized a new ligand, 2,6-bis{[(2-hydroxyphenyl)(2-pyridylmethyl)amino]methyl}-4-methylphenol (H_3L),[10] which contains mixed phenol and pyridine podands. In its coordinating form, H_3L is a trianionic, N_4O_3 donor ligand, which places it intermediate between the pentaanionic, N_2O_5 ligand HXTA and the monoanionic, N_6O ligands such as HMPA. Both diferric and dicobaltic complexes of this ligand have been characterized and are discussed here.

Table III. Selected Atomic Coordinates ($\times 10^4$) and Equivalent Isotropic Thermal Parameters (Å$^2 \times 10^3$) for $[LCo_2(OPr)_2]BPh_4$

	x	y	z	$U(eq)^a$
Co(1)	1675(1)	3590(1)	567(1)	37(1)
Co(2)	1020(1)	4149(1)	860(1)	35(1)
O(1)	1521(2)	4430(5)	971(2)	36(3)
O(2)	2097(2)	298395)	1137(2)	44(3)
O(3)	888(2)	5705(5)	691(2)	44(3)
O(4)	1421(2)	2159(5)	568(2)	43(3)
O(5)	1149(2)	2529(5)	1034(2)	39(3)
O(6)	1234(2)	4127(5)	−52(2)	45(3)
O(7)	782(2)	3813(5)	145(2)	44(3)
N(1)	198792)	4870(6)	561(3)	36(4)
N(2)	1825(2)	2863(7)	127(3)	40(4)
N(3)	1174(2)	4527(6)	1561(3)	34(4)
N(4)	538(2)	3804(6)	815(3)	38(4)
C(1)	1750(2)	5253(8)	1316(3)	32(4)
C(2)	1930(3)	6095(8)	1183(3)	41(5)
C(3)	2167(3)	6902(8)	1532(4)	45(5)
C(4)	2227(3)	6953(9)	2030(4)	52(6)
C(5)	2041(2)	6114(9)	2143(3)	46(5)
C(6)	1807(2)	5271(8)	1802(3)	35(4)
C(7)	2484(3)	7884(10)	2404(4)	72(7)
C(8)	1866(3)	6049(8)	658(3)	48(5)
C(9)	2384(3)	4565(8)	961(3)	39(5)
C(10)	2414(3)	3572(8)	1248(3)	38(5)
C(11)	2777(3)	3202(9)	1623(4)	53(5)
C(12)	3089(3)	3856(11)	1725(4)	61(6)
C(13)	3057(3)	4862(11)	1457(4)	57(6)
C(14)	2700(3)	5222(9)	1074(4)	51(6)
C(15)	1944(3)	4877(8)	50(3)	45(5)
C(16)	1952(3)	3643(9)	−93(3)	43(5)
C(17)	2053(3)	3271(9)	−437(3)	46(5)
C(18)	2031(3)	2107(10)	−558(4)	57(6)
C(19)	1912(3)	1336(9)	−320(3)	54(6)
C(20)	1809(3)	1736(9)	16(3)	48(5)
C(21)	1597(2)	4409(8)	1925(3)	40(4)
C(22)	1043(2)	5737(8)	1542(3)	39(5)
C(23)	908(2)	6283(3)	1080(3)	41(5)
C(24)	788(3)	7454(9)	1039(4)	57(6)
C(25)	806(3)	8014(10)	1449(5)	66(7)
C(26)	944(3)	7442(11)	1905(5)	67(7)
C(27)	1061(3)	6293(9)	1959(4)	51(5)
C(28)	963(2)	3694(8)	1707(3)	42(5)
C(29)	572(2)	3583(8)	1265(3)	38(5)
C(30)	256(3)	3266(9)	1296(4)	59(6)
C(31)	−98(3)	3207(10)	860(5)	68(7)
C(32)	−122(3)	3493(10)	409(4)	60(6)
C(33)	192(3)	3776(8)	383(4)	46(5)
C(34)	1295(2)	1857(9)	853(3)	41(5)
C(35)	1311(3)	566(9)	981(5)	74(8)
C(36)^b	1702(5)	159(18)	1311(9)	98(14)
C(37)	893(3)	3940(8)	−164(3)	46(5)
C(38)	605(3)	3886(11)	−733(4)	73(6)
C(39)^b	211(5)	3499(18)	−896(6)	88(11)
C(36A)^c	1485(14)	−206(42)	844(18)	105(14)
C(39A)^c	671(12)	2923(43)	−933(17)	113(15)

^{a} Equivalent isotropic U defined as one-third of the trace of the orthogonalized U_{ij} tensor. ^{b} 66% occupancy term. ^{c} 34% occupancy atom.

Experimental Section

General Procedures. All reagents and solvents were purchased from commercial sources and used as received, with the following exceptions: Methanol and acetonitrile were distilled from calcium hydride, tetrahydrofuran (THF) was distilled from sodium benzophenone ketyl, chloroform was distilled from calcium chloride, and dimethylformamide (DMF) was distilled from molecular sieves prior to use. 2,6-Bis(chloromethyl)-4-methylphenol was synthesized by the method of Borovik et al.[2b] 2-[[(o-Hydroxyphenyl)amino]methyl]pyridine was synthesized by the method of Pitt et al.[11]

Melting points were determined using a Thomas capillary melting point apparatus and are uncorrected. NMR spectra were obtained in CDCl$_3$, acetone-d_6 or DMSO-d_6 at 25 °C on a Bruker AC300 spectrometer. ^{19}F NMR spectra were referenced to CFCl$_3$ = δ 0.0. IR

(11) Pitt, C. G.; Bao, Y.; Thompson, J.; Wani, M. C.; Rosenkrantz, H.; Metterville, J. *J. Med. Chem.* **1986**, *29*, 1231.

Table IV. Selected Bond Distances (Å) and Angles (deg) for H₃L and [LCo₂(OPr)₂]BPh₄

Distances

	H₃L	[LCo₂(OPr)₂]-BPh₄		H₃L	[LCo₂(OPe)₂]-BPh₄		H₃L	[LCo₂(OPr)₂]-BPh₄
Co(1)-O(1)		1.908(7)	N(3)-C(21)	1.484(8)	1.505(9)	C(22)-C(23)	1.360(7)	1.38(1)
Co(1)-O(2)		1.846(5)	N(3)-C(22)	1.449(7)	1.47(1)	C(22)-C(27)	1.392(8)	1.39(2)
Co(1)-O(4)		1.937(6)	N(3)-C(28)	1.439(7)	1.50(1)	C(23)-C(24)	1.378(9)	1.41(1)
Co(1)-O(6)		1.928(5)	N(4)-C(29)	1.332(9)	1.33(1)	C(24)-C(25)	1.41(1)	1.38(2)
Co(1)-N(1)		1.947(8)	N(4)-C(33)	1.39(1)	1.352(9)	C(25)-C(26)	1.354(9)	1.37(2)
C(1)-N(2)		1.93(1)	C(1)-C(2)	1.399(9)	1.39(2)	C(26)-C(27)	1.397(9)	1.38(2)
Co(2)-O(1)		1.921(7)	C(1)-C(6)	1.390(7)	1.38(1)	C(28)-C(29)	1.530(9)	1.48(1)
Co(2)-O(3)		1.852(6)	C(2)-C(3)	1.388(8)	1.37(1)	C(29)-C(30)	1.377(9)	1.39(2)
Co(2)-O(5)		1.924(6)	C(2)-C(8)	1.503(7)	1.49(2)	C(30)-C(31)	1.39(1)	1.38(1)
Co(2)-O(7)		1.922(6)	C(3)-C(4)	1.390(8)	1.41(2)	C(31)-C(32)	1.38(1)	1.37(2)
Co(2)-O(7)		1.922(6)	C(4)-C(5)	1.39(1)	1.37(2)	C(32)-C(33)	1.34(1)	1.36(2)
Co(2)-N(3)		1.947(8)	C(4)-C(7)	1.507(8)	1.52(1)	C(34)-C(35)		1.52(2)
Co(2)-N(4)		1.939(8)	C(5)-C(6)	1.379(8)	1.38(1)	C(35)-C(36)		1.46(2)
O(1)-C(1)	1.371(7)	1.365(9)	C(6)-C(21)	1.502(9)	1.48(1)	C(35)-C(36A)		1.33(6)
O(2)-C(10)	1.345(8)	1.34(1)	C(9)-C(10)	1.375(9)	1.40(1)	C(37)-C(38)		1.52(1)
O(3)-C(23)	1.378(7)	1.32(1)	C(9)-C(14)	1.381(9)	1.37(2)	C(38)-C(39)		1.49(2)
O(4)-C(34)		1.27(2)	C(10)-C(11)	1.39(1)	1.40(1)	C(38)-C(39A)		1.35(6)
O(5)-C(34)		1.26(1)	C(11)-C(12)	1.38(1)	1.37(2)	O(1)···O(3)	2.803(7)	
O(6)-C(37)		1.27(1)	C(12)-C(13)	1.37(1)	1.38(2)	O(1)···N(1)	2.953(8)	
O(7)-C(37)		1.25(2)	C(13)-C(14)	1.38(1)	1.38(1)	O(1)···N(2)	2.860(8)	
N(1)-C(8)	1.468(7)	1.51(1)	C(15)-C(16)	1.52(1)	1.48(1)	O(2)···N(1)	2.731(8)	
N(1)-C(9)	1.440(9)	1.49(1)	C(16)-C(17)	1.352(9)	1.38(2)	O(2)···N(2)	3.130(8)	
N(1)-C(15)	1.470(7)	1.48(1)	C(17)-C(18)	1.38(1)	1.38(2)	O(3)···N(3)	2.731(8)	
N(2)-C(16)	1.333(9)	1.37(1)	C(18)-C(19)	1.38(1)	1.38(2)	O(4)···N(4)	2,813(9)	
N(2)-C(20)	1.35(1)	1.32(1)	C(19)-C(20)	1.34(1)	1.39(2)			

Angles

	[LCo₂(OPr)₂]BPh₄		H₃L	[LCo₂(OPe)₂]BPh₄		H₃L	[LCo₂(OPr)₂]BPh₄
O(1)-Co(1)-O(2)	92.1(3)	Co(1)-N(1)-C(9)		105.0(5)	C(12)-C(13)-C(14)	120.2(7)	119(1)
O(1)-Co(1)-O(4)	94.0(3)	C(8)-N(1)-C(9)	118.3(4)	112.0(6)	C(9)-C(14)-C(13)	119.7(6)	120(1)
O(2)-Co(1)-O(4)	85.6(3)	Co(1)-N(1)-C(15)		106.8(5)	N(1)-C(15)-C(16)	111.5(6)	107.3(8)
O(1)-Co(1)-O(6)	91.3(3)	C(8)-N(1)-C(15)	112.1(5)	109.0(7)	N(2)-C(16)-C(15)	115.0(6)	114(1)
O(2)-Co(1)-O(6)	176.1(3)	C(9)-N(1)-C(15)	114.2(5)	111.1(8)	N(2)-C(16)-C(17)	122.6(7)	120.7(9)
O(4)-Co(1)-O(6)	92.2(2)	Co(1)-N(2)-C(16)		113.5(6)	C(15)-C(16)-C(17)	122.4(6)	120.7(9)
O(1)-Co(1)-N(1)	93.6(3)	Co(1)-N(2)-C(16)		127.2(8)	C(16)-C(17)-C(18)	119.5(7)	120(1)
O(2)-Co(1)-N(1)	89.6(3)	Co(16)-N(2)-C(20)	117.6(7)	119(1)	C(17)-C(18)-C(19)	118.3(7)	118(1)
O(4)-Co(1)-N(1)	171.1(3)	Co(2)-N(3)-C(21)		113.3(6)	C(18)-C(19)-C(20)	118.9(9)	120(1)
O(6)-Co(1)-N(1)	92.2(3)	Co(2)-N(3)-C(22)		105.0(5)	N(2)-C(20)-C(19)	123.1(8)	121(1)
O(1)-Co(1)-N(2)	175.0(3)	C(21)-N(3)-C(22)	112.0(4)	111.7(4)	N(3)-C(21)-C(6)	112.(4)	110.3(7)
O(2)-Co(1)-N(2)	91.2(3)	Co(2)-N(3)-C(28)		106.0(5)	N(3)-C(22)-C(23)	116.4(5)	114.2(9)
O(4)-Co(1)-N(2)	89.9(3)	C(21)-N(3)-C(28)	114.8(4)	109.9(6)	N(3)-C(22)-C(27)	123.8(4)	123.0(8)
O(6)-Co(1)-N(2)	85.5(3)	C(22)-N(3)-C(28)	115.9(5)	110.6(8)	C(23)-C(22)-C(27)	119.7(5)	122.7(9)
N(1)-Co(1)-N(2)	82.8(4)	Co(2)-N(4)-C(29)		113.5(5)	C(3)-C(23)-C(22)	121.7(6)	120.3(8)
O(1)-Co(2)-O(3)	91.1(3)	Co(2)-N(4)-C(29)		113.5(5)	O(3)-C(23)-C(24)	117.1(5)	122.4(9)
O(1)-Co(2)-O(5)	89.8(3)	Co(29)-N(4)-C(33)	116.1(6)	120.4(9)	C(22)-C(23)-C(24)	121.1(6)	117(1)
O(3)-Co(2)-O(5)	179.1(3)	O(1)-C(1)-C(2)	121.6(5)	120.4(9)	C(23)-C(24)-C(25)	118.8(5)	121(1)
O(1)-Co(2)-O(7)	96.1(3)	O(1)-C(1)-C(6)	116.0(5)	120.8(9)	C(24)-C(25)-C(26)	120.7(7)	120(1)
O(3)-Co(2)-O(7)	88.3(3)	C(2)-C(1)-C(6)	122.3(5)	118.8(8)	C(25)-C(26)-C(27)	119.5(6)	121(1)
O(5)-Co(2)-O(7)	91.7(3)	C(1)-C(2)-C(3)	117.5(5)	118.8(8)	C(22)-C(27)-C(26)	120.0(5)	118(1)
O(1)-Co(2)-N(3)	93.0(3)	C(1)-C(2)-C(8)	121.3(5)	117.7(8)	N(3)-C(28)-C(29)	111.5(4)	107.3(7)
O(3)-Co(2)-N(3)	88.7(3)	C(3)-C(2)-C(8)	121.2(6)	122(1)	N(4)-C(29)-C(28)	114.2(5)	115.0(9)
O(5)-Co(2)-N(3)	91.2(3)	C(2)-C(3)-C(4)	122.3(6)	122(1)	N(4)-C(29)-C(30)	124.4(6)	120.7(7)
O(7)-Co(2)-N(3)	170.4(3)	C(3)-C(4)-C(5)	117.4(6)	115.5(8)	C(28)-C(29)-C(30)	121.3(6)	124.3(9)
O(1)-Co(2)-N(4)	174.4(3)	C(3)-C(4)-C(7)	121.0(6)	121(1)	C(29)-C(30)-C(31)	119.4(7)	120(1)
O(3)-Co(2)-N(4)	92.1(3)	C(5)-C(4)-C(7)	121.6(5)	124(1)	C(30)-C(31)-C(32)	115.9(8)	117(1)
O(5)-Co(2)-N(4)	87.0(3)	C(4)-C(5)-C(6)	123.1(5)	124(1)	C(31)-C(32)-C(33)	123(1)	121.9(8)
O(7)-Co(2)-N(4)	88.6(3)	C(1)-C(6)-C(5)	117.4(6)	120(1)	N(4)-C(33)-C(32)	121.1(9)	120(1)
N(3)-Co(2)-N(4)	82.5(3)	C(1)-C(6)-C(21)	121.8(5)	117.7(7)	O(4)-C(34)-C(5)		125.9(9)
Co(1)-O(1)-Co(2)	118.5(3)	C(5)-C(6)-C(21)	120.8(5)	122.7(9)	O(4)-C(34)-C(35)		118(1)
Co(1)-O(1)-C(1)	121.6(6)	N(1)-C(8)-C(2)	111.8(5)	110.2(7)	O(5)-C(34)-C(35)		116(1)
Co(2)-O(1)-C(1)	119.9(6)	N(1)-C(9)-C(10)	117.2(6)	114.4(8)	C(34)-C(35)-C(36)		112(1)
Co(1)-O(2)-C(10)	111.3(5)	N(1)-C(9)-C(14)	122.8(6)	124.4(8)	C(34)-C(35)-C(36A)		122(3)
Co(2)-O(3)-C(23)	110.7(6)	C(10)-C(9)-C(14)	120.0(6)	121.0(7)	O(6)-C(37)-O(7)		126.1(8)
Co(1)-O(4)-C(34)	129.6(6)	O(2)-C(10)-C(9)	121.1(7)	119.1(7)	O(6)-C(37)-C(38)		114(1)
Co(2)-O(5)-C(34)	126.0(7)	O(2)-C(10)-C(11)	118.6(7)	122.4(9)	O(7)-C(37)-C(38)		120(1)
Co(1)-O(6)-C(37)	123.8(7)	C(9)-C(10)-C(11)	120.4(7)	118(1)	O(37)-C(38)-C(39)		118(1)
Co(2)-O(7)-C(37)	132.0(5)	C(10)-C(11)-C(12)	119.1(7)	120(1)	C(37)-C(38)-C(39A)		110(2)
Co(1)-N(1)-C(8)	112.8(7)	C(11)-C(12)-C(13)	120.6(8)	121.8(9)	O(39)-C(38)-C(39A)		92(2)

spectra were recorded on a Nicolet 5 DX FTIR spectrometer using KBr pellets. Electronic absorption spectra were measured on a Shimadzu UV-3100 spectrophotometer in DMF or acetonitrile solution. Cyclic voltammograms were also determined in DMF or acetonitrile with 0.1 M tetrabutylammonium hexafluorophosphate as the supporting electrolyte. A PAR 273 potentiostat with a platinum-disk working electrode, a platinum-wire auxiliary electrode, and a SCE reference electrode were used. The ferrocenium/ferrocene couple was included as an internal standard. Mössbauer data were obtained on an Austin S-600 and were referenced to metallic iron foil. Elemental analyses were performed by Atlantic Microlabs, Atlanta, GA.

2,6-Bis{[(2-hydroxyphenyl)(2-pyridylmethyl)amino]methyl}-4-methylphenol (H₃L). A solution containing 9.38 g of 2-[[(o-hydroxyphenyl)amino]methyl]pyridine (0.047 mol) and 9.48 g of triethylamine (0.094

mol) in 25 mL of THF was slowly dripped into a solution of 4.82 g of 2,6-bis(chloromethyl)-4-methylphenol (0.024 mol) in 115 mL of THF at 0 °C. The reaction mixture was warmed to room temperature and stirred for 4 days. The mixture was then filtered, and the resulting solid was washed with methylene chloride. The combined organic fractions were rotoevaporated, and the resulting solid was triturated with hexane. In this manner, 12.1 g (93%) of $H_3L\cdot^1/_2H_2O$ was obtained as a reddish solid, mp 131–132 °C. Anal. Calcd for $H_3L\cdot^1/_2H_2O$, $C_{33}H_{33}N_4O_{3.5}$: C, 73.18; H, 6.14. Found: C, 73.00; H, 6.14. ^1H NMR (CDCl$_3$): δ 9.93 (br s, 2H, OH), 8.58 (dd, 2H, Ar H (py)), 7.41 (ddd, 2H, Ar H (py)), 7.17 (dd, 2H, Ar H (aminophenol)), 7.11 (ddd, 2H, Ar H (py)), 6.96 (ddd, 2H, Ar H (aminophenol)), 6.91 (dd, 2H, Ar H (py)), 6.88 (dd, 2H, Ar H (aminophenol)), 6.75 (ddd, 2H, Ar H (aminophenol)), 6.66 (s, 2H, Ar H (cresol)), 5.11 (br s, 1H, OH), 4.13 (s, 4H, NCH$_2$), 4.11 (s, 4H, NCH$_2$), 1.99 (s, 3H, CH$_3$). IR (KBr), cm^{-1}: 3070 (OH str), 3052, 2923, 2853 (C—H str), 1599, 1493, 1441 (C=C, C=N str), 1364 (O—H bend), 1259 (C—O str), 749 (H—C=C bend). Red, X-ray-quality crystals were obtained by crystallization from methylene chloride–hexane.

Bis(μ-propionato-O,O')(2,6-bis{[(2-phenoxy)(2-pyridylmethyl)amino]methyl}-4-methylphenolato)diiron(III) Tetrafluoroborate, [LFe$_2$(OPr)$_2$]BF$_4$. A solution containing 140 mg of H$_3$L (0.26 mmol) and 104 mg of FeCl$_2$·4H$_2$O (0.52 mmol) or 122 mg of FeCl$_3$·4H$_2$O (0.52 mmol) in 15 mL of methanol was stirred at room temperature. After 30 min, 105 mg of NaOPr (1.56 mmol) was added, followed by 57.1 mg of NaBF$_4$ (0.52 mmol) after an additional 30 min. Stirring was continued for 1 h; then the solution was evaporated to dryness, and the resulting solid was extracted with water. The purple water layer was reextracted with methylene chloride, yielding a dark blue solution. This solution was concentrated and layered with hexane to yield 87.0 mg (32% yield) of dark blue crystals, mp >210 °C. Anal. Calcd for [LFe$_2$(OPr)$_2$]-BF$_4$·2CH$_2$Cl$_2$, $C_{41}H_{43}BCl_4F_4Fe_2N_4O_7$: C, 47.16; H, 4.15. Found: C, 47.16; H, 4.03. ^1H NMR (CDCl$_3$): δ 78, 69, 66, 52, 48, 15, –42, –59. IF (KBr), cm^{-1}: 1564, 1481, 1432 (C=C, C=N str), 1284 (C—O str), 754 (H—C=C bend). UV (DMF): 501 nm. CV (DMF), $E_{1/2}$: –0.18, –0.81 V vs SCE.

Bis(μ-propionato-O,O')(2,6-bis{[(2-phenoxy)(2-pyridylmethyl)amino]methyl}-4-methylphenolato)diiron(III) Tetraphenylborate, [LFe$_2$(OPr)$_2$]BPh$_4$. Synthesis of this complex was carried out as above, but with the following workup: The reaction mixture was filtered, and the resulting dark solid was washed with benzene until the benzene washings remained colorless. The solid was then crystallized by diffusion of hexane into a chloroform solution. The dark blue crystals were washed with water and dried under vacuum, yielding 50 mg of the product (17% yield). Anal. Calcd for [LFe$_2$(OPr)]BPh$_4$·H$_2$O, $C_{63}H_{63}BFe_2N_4O_8$: C, 67.28; H, 5.47. Found: C, 67.22; H, 5.62. CV (DMF), $E_{1/2}$: –0.18, –0.82 V vs SCE. CV (CH$_3$CN), $E_{1/2}$: –0.14, –0.76 V vs SCE.

Bis(μ-propionato-O,O')(2,6-bis{[(2-phenoxy)(2-pyridylmethyl)amino]methyl}-4-methylphenolato)dicobalt(III) Tetraphenylborate, [LCo$_2$(OPr)$_2$]BPh$_4$. A solution containing 160 mg of H$_3$L (0.30 mmol), 142 mg of CoCl$_2$·6H$_2$O (0.60 mmol), and 86 mg of NaOPr (0.90 mmol) was refluxed in 30 mL of methanol. After 4 h, 205 mg of NaBPh$_4$ (0.60 mmol) was added, and reflux was continued for an additional 2 h. The solution was filtered, and the filtrate was cooled, causing precipitation of the complex as a red solid. Recrystallization from chlorobenzene/acetonitrile gave 42 mg (11% yield) of dark red crystals, mp >210 °C. Anal. Calcd for [LCo$_2$(OPr)$_2$]BPh$_4$·C$_6$H$_5$Cl, $C_{69}H_{64}BClCo_2N_4O_7$: C, 67.63 H, 5.26. Found: C, 67.31; H, 5.28. IR (KBr), cm^{-1}: 1568, 1481, 1426 (C=C, C=N str), 1291 (C—O str), 746 (H—C=C bend). UV (CH$_3$CN): 457 nm. CV (DMF), E_p: –0.19, –0.77 V vs SCE.

Bis(μ-propionato-O,O')(2,6-bis{[(2-phenoxy)(2-pyridylmethyl)amino]methyl}-4-methylphenolato)dicobalt(III) Tetrafluoroborate, [LCo$_2$(OPr)$_2$]BF$_4$. Synthesis of this complex was carried out as above, but with the following workup: The reaction mixture was evaporated to dryness, and the solid was dissolved in 1:1 chloroform/acetone. The resulting solution was washed with water, followed by removal of the solvent. The solid was then triturated with hexanes and dried, yielding 32 mg of a brown solid (12% yield). Anal. Calcd for [LCo$_2$(OPr)$_2$]-BF$_4$·H$_2$O, $C_{39}H_{41}BCo_2F_4N_4O_8$: C, 52.14; H, 4.60. Found: C, 51.79; H, 4.77. ^{19}F NMR (CDCl$_3$): δ 152.9.

X-ray Structure Analyses. Intensity measurements were made at room temperature (21 °C) on a Nicolet R3mV diffractometer with graphite-monochromated Mo Kα radiation (λ = 0.710 73 Å). Relevant crystallographic data are listed in Table I. Cell parameters were based on 49 reflections with 2θ values ranging from 26.7 to 40.7° for H$_3$L and 38 reflections with 2θ values ranging from 24.1 to 35.2° for [LCo$_2$-(OPr)$_2$]BPh$_4$. Data were measured to 2θ = 45° using ω/2θ scans for
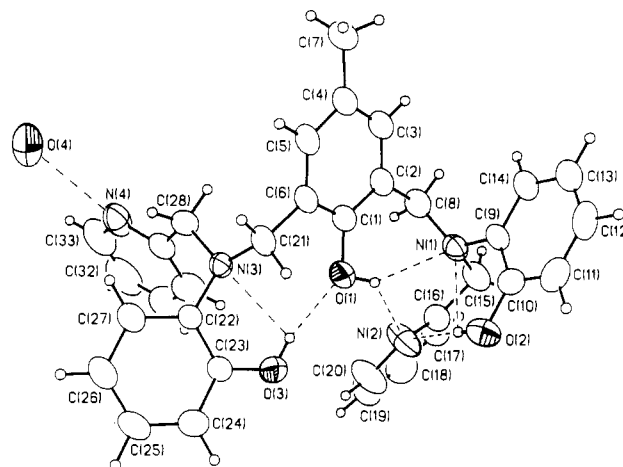

Figure 1. Thermal ellipsoid plot (35% probability ellipsoids) of the H$_3$L ligand showing the atom-numbering scheme used.

H$_3$L and ω scans for [LCo$_2$(OPr)$_2$]BPh$_4$. Periodic measurement of three standard reflections indicated crystal and electronic stability (±2%). Lorentz and polarization corrections and an empirical absorption correction were applied for both compounds.

The structures were solved by direct methods and refined by full-matrix least-squares techniques using the SHELXTL+ package of programs. The lattice of H$_3$L contains a water molecule which is crystallographically disordered over two equivalent sites related by an inversion center at $(0, ^1/_2, ^1/_2)$. The lattice of [LCo$_2$(OPr)$_2$]BPh$_4$ contains two unique chlorobenzene solvent molecules; one is disordered about a 2-fold rotation axis $(^1/_2, y, ^1/_4)$, and the other is disordered about an inversion center $(0, 0, 0)$. In addition, the alkyl chains of each of the propionate ligands are disordered over two possible sites, each of which are related by rotation about the C–CH$_2$ bond. For both propionate ligands, the major component occupancy refined to a value of $m = 0.66$ and was constrained to this value in the final least-squares cycles; the minor component occupancy was set equal to $1 - m$. All non-hydrogen atoms of H$_3$L were refined anisotropically. Only the non-hydrogen ordered or major component atoms of the cation in [LCo$_2$(OPr)$_2$]BPh$_4$ were refined anisotropically; all others were refined with isotropic thermal parameters. Hydrogen atoms, other than those of the methyl group of the H$_3$L ligand in the complex, the disordered propionate ligands, or solvent molecules, were located by standard difference Fourier techniques and included in the structure factor calculation at optimized positions.

Positional parameters for the atoms of H$_3$L and important atoms of [LCo$_2$(OPr)$_2$]BPh$_4$ are given in Tables II and III. Selected bond distances and angles for both compounds are given in Table IV. Tables giving full experimental details (Tables S1 and S5), positional parameters for all atoms (Table S6), complete distances and angles (Tables S2 and S7), anisotropic thermal parameters (Tables S3 and S8), and optimized hydrogen atom coordinates (Tables S4 and S9) are available as supplementary material.
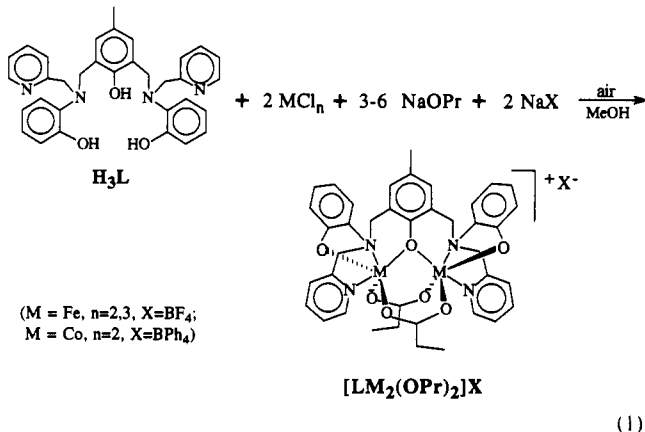
Results and Discussion

Ligand. The ligand, H$_3$L, was synthesized in high yield by nucleophilic displacement of the chlorides from 2,6-bis(chloromethyl)-p-cresol by 2-[[(o-hydroxyphenyl)amino]methyl]pyridine. The ligand produced red cubic crystals upon slow diffusion of hexane into a methylene chloride solution.

The structure of the H$_3$L ligand is shown in Figure 1. Atomic coordinates and bonding distances are provided in Tables II and IV, respectively. The molecular conformation of H$_3$L is dominated by extensive, but weak, intramolecular and intermolecular hydrogen bonding (indicated as dashed lines in Figure 1.)

Diiron Complexes. The protonated form of the ligand was used in all syntheses and reacted rapidly with the iron source.

(12) The iron(II)-containing complexes obtained in the absence of oxygen exhibit sharp peaks over a range from –90 to +350 ppm, which is consistent with the presence of high-spin iron(II). In contrast, the diferric complex, [Fe$_2$L(OPr)$_2$]$^+$, exhibits broad resonances ranging from –60 to +80 ppm, which is indicative of high-spin iron(III) complexes, with no iron(II) present. Bertini, I.; Luchinat, C. *NMR of Paramagnetic Molecules in Biological Systems*; Benjamin/Cummings: Menlo Park, CA, 1986.

Addition of iron(III) chloride and sodium propionate to the ligand, in either the presence or the absence of oxygen, immediately resulted in the dark blue $Fe^{III}Fe^{III}$ complex, $[Fe_2L(OPr)_2]^+$ (eq 1). Unlike the iron(III) chloride, iron(II) chloride reacted with

$$H_3L + 2 MCl_n + 3\text{-}6 \ NaOPr + 2 \ NaX \xrightarrow[\text{MeOH}]{\text{air}}$$

(M = Fe, n=2,3, X=BF$_4$;
M = Co, n=2, X=BPh$_4$)

$[LM_2(OPr)_2]X$

(1)

the ligand in the absence of oxygen to produce a brown solution. This complex incorporated one or more iron(II) centers both before and after addition of sodium propionate, as determined by proton NMR analysis of the products formed.[12] The Fe^{II} in these complexes is readily oxidized to Fe^{III} in the presence of oxygen. Consequently, when the reaction was carried out in an oxygen-containing atmosphere, no Fe^{II} complexes were observed.

The complex $[Fe_2L(OPr)_2]^+$ exhibits a stable, triply-bridged diiron core consisting of two propionates and a bridging phenoxide.[13] (μ-Oxo)- or (μ-phenoxo)bis(μ-carboxylato)diiron cores are common to diiron complexes of this type and have been observed for a number of $Fe^{III}Fe^{III}$ and $Fe^{II}Fe^{III}$ complexes.[1b-e,2-4a,14] Acetates or benzoates readily coordinated in place of the propionates, but attempts to replace these carboxylato groups with neutral ligands, such as DMF or acetamide, were unsuccessful. The complexes were isolated with either BF_4^- or BPh_4^- as the counterion. The tetrafluoroborate salt, $[Fe_2L(OPr)_2]BF_4$, was water soluble, while the tetraphenylborate salt, $[Fe_2L(OPr)_2]BPh_4$, was not.

The Mössbauer spectrum of $[Fe_2L(OPr)_2]BF_4$ as a solid at 298 K exhibits a quadrupolar doublet with an isomer shift of $\delta = 0.37$ μm/s and a quadrupole splitting of $\Delta E_Q = 0.77$ mm/s (Figure S1, available as supplementary material). This indicates a single type of high-spin iron(III) center and is consistent with a high-spin $Fe^{III}Fe^{III}$ complex.[15] The related diferric complex

$[Fe_2(LBzim)(OAc)_2](ClO_4)_3$ exhibits a similar Mössbauer spectrum at 77 K with δ and ΔE_Q values of 0.27 mm/s and 0.71 mm/s, respectively.[1c]

The two phenoxide podands on the ligand appear to be primarily responsible for the ease with which both irons are oxidized to iron(III). Cyclic voltammetry indicates that oxidation to the $Fe^{III}Fe^{III}$ state is facile, with an $E_{1/2}$ of -0.14 V versus SCE in acetonitrile for the $Fe^{III}Fe^{III}/Fe^{II}Fe^{III}$ couple of $[Fe_2L(OPr)_2]$-(BPh$_4$). This is in contrast to the related $Fe^{II}Fe^{III}$ complex $[Fe_2(BPMP)(OPr)_2](BPh_4)_2$, reported by Que.[2b] The BPMP complex, in which all the ligand podands are pyridines, is readily reduced from the $Fe^{III}Fe^{III}$ to the $Fe^{II}Fe^{III}$ form, with an $E_{1/2}$ of $+0.69$ V versus SCE in acetonitrile for the $Fe^{III}Fe^{III}/Fe^{II}Fe^{III}$ couple. Stabilization of the $Fe^{II}Fe^{III}$ state was also observed for the related imidazolyl[3] and benzimidazolyl[1c] complexes $[Fe_2$-(Bimp)(RCO$_2$)$_2$](X)$_2$ (R = CH$_2$CH$_3$, CH$_3$; X = BPh$_4$, BF$_4$) and $[Fe_2(LBzim)(RCO_2)_2](BF_4)_2$ (R = C$_6$H$_5$, CH$_3$), respectively.
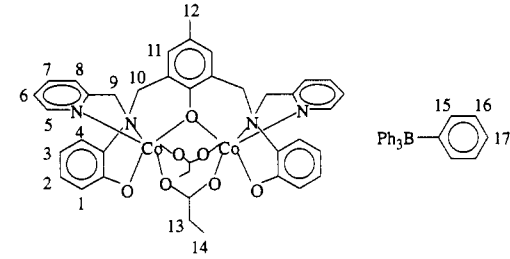
Dicobalt Complexes. Reaction of cobalt(II) chloride and sodium propionate with the protonated ligand resulted in a complex which was shown to be paramagnetic by ^{1}H NMR. This indicates that at least one cobalt remained in the $+2$ oxidation state. No more paramagnetic species were observed by NMR following reflux of this complex in methanol under an atmosphere of air for 24 h, indicating that the cobalt was completely oxidized to diamagnetic cobalt(III). Addition of NaBF$_4$ or NaBPh$_4$ enhanced the rate of oxidation, and no paramagnetic cobalt species remained after a total of 6 h reflux. This overall oxidation is much slower than that observed for the analogous iron complexes. The dicobaltic complex $[Co_2L(OPr)_2]X$ (X = BF$_4$, BPh$_4$) was isolated from the final reaction mixture (eq 1).

Cyclic voltammograms of $[Co_2L(OPr)_2]BPh_4$ in DMF showed irreversible reduction peaks at -0.19 and -0.77 V which rapidly decreased in intensity with repeated scans. These reduction potentials are similar to those observed for the analogous iron complex (-0.21 and -0.86 V); however, the irreversibility of the cobalt system makes direct comparison of the oxidation potentials impossible. The lack of observed cobalt oxidation peaks corroborates the less facile oxidation process observed during formation of the cobalt complex. Both the electrochemical irreversibility and the slow chemical oxidation of the cobalt complex are most likely due to the electronic redistribution and geometric rearrangements which typically accompany oxidation of a cobalt center from the $+2$ to the $+3$ oxidation state.

No dioxygen complexes were isolated, even though oxidation of the cobalt occurred in the air. This is unlike the case of the dicobaltous complexes of the HBPMP polypodal ligand, from which dioxygen adducts were isolated following air oxidation. The oxygen affinity of these related complexes was shown to be proportional to the electron density on the cobalt.[6] The ligand L, with its N$_2$O$_2$ donor set for each cobalt and five-membered chelate rings, should be sufficiently electron donating to allow dioxygen adduct formation.[16] However, dioxygen coordination by the reported dicobaltous complexes occurs in a μ-peroxo fashion, which requires an open coordination site on each cobalt. Maintenance of this open coordination site in our complex prior to oxidation is inhibited by the presence of an excess of sodium propionate, which was necessary to avoid decomplexation of the cobalt. Once oxidation occurs, the reduced electron density on the cobaltic centers most likely inhibits the complex's affinity for dioxygen.

The oxidized, diamagnetic cobalt(III) complexes $[Co_2L$-(OPr)$_2$]X (X = BF$_4$, BPh$_4$) exhibited ^{1}H NMR spectra which were counterion dependent in chloroform solution. These spectra converged with increasing solvent polarity until they became

(13) The structure determination of the complex $[Fe_2L(OPr)_2]BF_4$ was hampered by a badly disordered anion and by ambiguity in the location of the anion and a badly disordered chloroform solvent molecule. As the original room-temperature data set indicated significant crystal decomposition over the course of the experiment, probably due to solvent loss, a second data set was collected at -70 °C. Unfortunately, these data were plagued by similar problems and did not produce a model suitable for detailed analysis. However, both were sufficient to verify that the molecular shape of the cation is similar to that of the cobalt complex. Crystal data for $[Fe_2(OPr)_2]BF_4\cdot CHCl_3$ (monoclinic space group $P2_1/n$ (No. 14); Z = 4): at T = 294 K, a = 14.701(8) Å, b = 20.42(1) Å, c = 17.388(7) Å, β = 101.73(4)°, V = 5111(4) Å^3, and Z = 4; at T = 203 K, a = 14.335(9) Å, b = 20.060(9) Å, c = 17.209(9) Å, β = 101.00(5)°, and V = 4857(5) Å^3. Crystals of the complex were obtained as the nitrate, tetraphenylborate, and hexafluorophosphate salts in addition to the tetrafluoroborate salt. Of these, the tetrafluoroborate salt exhibited the greatest degree of order.

(14) (a) Gomez-Romero, P.; Casan-Pastor, N.; Ben-Hussein, A.; Jameson, G. B. *J. Am. Chem. Soc.* **1988**, *110*, 1988. (b) Toftlund, H.; Murray, K. S.; Zwack, P. R.; Taylor, L. F.; Anderson, O. P. *J. Chem. Soc., Chem. Commun.* **1986**, 191. (c) Spool, A.; Williams, I. D.; Lippard, S. J. *Inorg. Chem.* **1985**, *24*, 2156. (d) Armstrong, W. H.; Spool, A.; Papaefthymiou, G. C.; Frankel, R. B.; Lippard, S. J. *J. Am. Chem. Soc.* **1984**, *106*, 3653.

(15) (a) *Mössbauer Spectroscopy*; Dickson, D. P. E., Berry, F. J., Eds.; Cambridge University Press: Cambridge, U.K., 1986. (b) Greenwood, N. N.; Gibb, T. C. *Mössbauer Spectroscopy*; Chapman and Hall: London, 1971.

(16) (a) Timmons, J. H.; Niswander, R. H.; Clearfield, A.; Martell, A. E. *Inorg. Chem.* **1979**, *18*, 2977. (b) Harris, W. R.; Murase, I.; Timmons, J. H.; Martell, A. E. *Inorg. Chem.* **1979**, *17*, 889. (c) McLendon, G.; Martell, A. E. *J. Chem. Soc., Chem. Commun.* **1975**, 223.

Table V. Solvent Dependence of the Proton NMR Shifts for [Co$_2$L(OPr)$_2$]X (X = BF$_4$, BPh$_4$)

		solvent			
CDCl$_3$		(CD$_3$)$_2$CO		DMSO-d_6	
X = BF$_4$	X = BPh$_4$	X = BF$_4$	X = BPh$_4$	X = BF$_4$	X = BPh$_4$
1^a 7.49^b	6.97	7.58	7.56	7.56	7.56
2 6.31	6.29	6.29	6.29	6.28	6.24
3 6.50	6.50	6.49	6.52	6.48	6.46
4 6.33	6.35	6.28	6.28	6.21	6.21
5 8.65	8.58	8.79	8.80	8.59	8.60
6 7.37	7.30	7.66	7.65	7.61	7.59
7 7.80	7.63	8.07	8.08	8.02	8.05
8 7.62	6.89	7.70	7.69	7.64	7.68
9 5.53	5.16	5.58	5.72	5.46	5.49
4.94	3.99	4.78	4.86	4.72	4.75
10 4.53	4.38	4.45	4.54	4.37	4.32
3.70	3.19	3.72	3.73	3.74	3.73
11 6.28	6.22	6.40	6.41	6.34	6.36
12 1.66	1.71	1.71	1.68	1.63	1.66
13 2.72	2.68	2.79	2.78	2.70	2.71
14 1.01	1.00	1.03	1.07	0.92	0.95
15	7.51		7.34		7.16
16	7.06		6.92		6.90
17	6.92	6.75			6.77

^{a} Numbered proton positions as shown in accompanying structure.
^{b} Proton shifts in ppm relative to solvent as the standard.

identical in DMSO. Data for the samples in chloroform-d_1, acetone-d_6, and DMSO-d_6 are shown in Table V. The solvent dependence of the proton shifts was more pronounced for the BPh$_4^-$ counterion and appears to be due to an ion-pairing interaction with the complex. Neither the ^{1}H nor ^{19}F NMR shifts of the respective counterions showed any evidence of direct bonding to the cobalt. Proton shift assignments were made on the basis of 2D NMR COSY experiments.

X-ray Structure of [Co$_2$L(OPr)$_2$]BPh$_4$. Crystals suitable for X-ray diffraction analysis were obtained for [Co$_2$L(OPr)$_2$]BPh$_4$ by slow diffusion of chlorobenzene into an acetonitrile solution of the complex. The cobalt dimer (shown in Figure 2) possesses a pseudo-C_2 axis which passes through the long axis of the bridging phenolate group. The octahedral coordination spheres of the cobalt atoms are virtually identical.

The Co–O and Co–N distances are, in general, consistent with those of related structures,[6b,17] although the Co–O distances to the nonbridging phenolate groups are slightly shorter than the average value of 1.89(1) Å.[17] Bonding distances in the ligand vary little from those of the uncomplexed molecule; variations in the bonding angles occur, as expected. For example, there is a significant reduction in the bond angles of atoms N(1) and N(3), due to the increased pyramidalization which occurs on binding
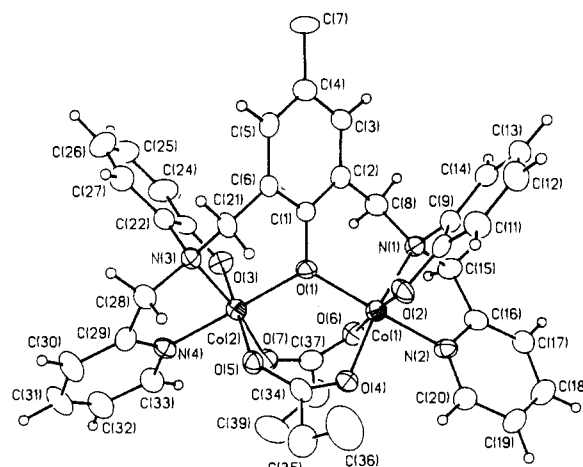
Figure 2. Thermal ellipsoid plot (35% probability ellipsoids) of the [LCo$_2$(OPr)$_2$]$^+$ cation showing the atom-numbering scheme used.

to the metal. On the other hand, the ring angles at atoms N(2) and N(4) expand, due to the decreased steric bulk of the lone pair when bound by the metal atoms.

Comparison of the free-ligand and complex structures reveals that an inversion at one of the tertiary amine junctures accompanies complexation of the ligand. This results in a ligand paddle wheel effect, similar to that observed in iron and cobalt complexes of other polypodal ligands.[1a,b,2,3a,5] The complex also contains a (μ-phenoxo)bis(μ-carboxylato)dicobalt core which is directly analogous to the triply-bridged diiron core. This arrangement has been observed in other dicobalt complexes of polypodal ligands, as well.[5]

Summary

Reaction of 2 equiv of iron(II) or cobalt(II) and propionate with the mixed donor, binucleating ligand H$_3$L resulted in an iron(II)- or cobalt(II)-containing complex, respectively. These compounds underwent oxidation to the singly charged, diferric or dicobaltic complexes, [M$_2$L(OPr)$_2$]$^+$ (M = Co, Fe). Oxidation was very rapid in the case of the iron complex but required 6–24 h for the cobalt complex. The diferric complex was also synthesized directly from 2 equiv of iron(III). In either case, a comparison of the free and coordinated ligands revealed an inversion at one of its tertiary amine junctures. A (μ-phenoxo)bis(μ-carboxylato)dimetal core was obtained in both the iron and cobalt complexes, in accordance with other reported complexes of this type. Single-crystal structures were obtained for the ligand, H$_3$L, and the dicobalt complex, [Co$_2$L(OPr)$_2$]BPh$_4$. Disordered crystals were obtained for the diiron complex, [Fe$_2$L(OPr)$_2$]BF$_4$, which nevertheless corroborated the similarity of this complex to that of its cobalt analogue.

Supplementary Material Available: Tables giving full crystallographic experimental details (Tables S1 and S5), positional parameters for all atoms (Table S6), complete distances and angles (Tables S2 and S7), anisotropic thermal parameters (Tables S3 and S8), and optimized hydrogen atom coordinates (Tables S4 and S9), a packing diagram of [Co$_2$L(OPr)$_2$]BPh$_4$ (Figure S1), and the ^{57}Fe Mössbauer spectrum of [Fe$_2$L(OPr)$_2$]BF$_4$ (Figure S2) (14 pages). Ordering information is given on any current masthead page.

(17) (a) Kistenmacher, T. J.; Marzilli, L. G.; Marzilli, P. A. *Inorg. Chem.* **1974,** *13,* 2089. (b) Bailey, N. A.; Higson, B. M.; McKenzie, E. D. *J. Chem. Soc., Dalton Trans.* **1972,** 503. (c) Calligaris, M.; Manzini, G.; Nardin, G.; Randaccio, L. *J. Chem. Soc., Dalton Trans.* **1972,** 543. (d) Calligaris, M.; Nardin, G.; Randaccio, L. *J. Chem. Soc., Dalton Trans.* **1972,** 1433.